Appl Phys B (2010) 101: 315–319
DOI 10.1007/s00340-010-4140-5

Applied Physics B
Lasers and Optics

Formation of InAs quantum dots in silicon by sequential ion implantation and flash lamp annealing

S. Prucnal · M. Turek · A. Drozdziel · K. Pyszniak · S.Q. Zhou · A. Kanjilal · W. Skorupa · J. Zuk

Received: 8 January 2010 / Revised version: 27 May 2010 / Published online: 17 July 2010

Abstract InAs quantum dots (QDs) were successfully formed in single-crystalline Si by sequential ion implantation and subsequent milliseconds range flash lamp annealing (FLA). Samples were characterized by μ-Raman spectroscopy, Rutherford Backscattering Spectrometry (RBS) high-resolution transmission electron microscopy (HRTEM) and low temperature photoluminescence (PL). The Raman spectrum shows two peaks at 215 and 235 cm^{-1} corresponding to the transverse optical (TO) and longitudinal optical (LO) InAs phonon modes, respectively. The PL band at around 1.3 μm originates from the InAs QDs with an average diameter 7.5 ± 0.5 nm and corresponds to the increased band gap energy due to the strong quantum confinement size effect. The FLA of 20 ms is sufficient for InAs QDs formation. It also prevents the out-diffusion of implanted elements. Moreover, the silicon layer amorphized during ion implantation is recrystallized by solid-phase epitaxial regrowth during FLA.

1 Introduction

Semiconductor nanoparticles are currently of great interest due to their wide potential applications in electrical and optoelectronic devices. From the optical point of view quantum dots (QDs) are interesting due to the possibility of tuning light emission by controlling the size-dependent quantum confinement effect, which modifies the bulk electronic band structure. This effect determines the strong size-dependent shift both in the optical band gap and in the exciton binding energy when a QD size (R) is of the order of the excitonic Bohr radius a_b [1–3]. The strong confinement occurs when $R \ll a_b$. Recently, extensive investigations were focused on optical and electrical properties of the films containing different semiconductor nanoparticles. Silicon with its indirect band gap is a poor light emitter but many devices like light emitting diodes (LEDs) [4], non-volatile memories [5] or solar cells [6] have been fabricated based on the silicon nanocrystals (Si-nc) embedded in silica or silicon nitride films. Beside Si-nc, several III–V and II–VI semiconductor nanocrystals have been successfully formed in different hosts. The main fabrication methods for such QDs are porous glass method [7], vapor deposition [8], radio frequency co-sputtering [9], sol-gel synthesis [10] and ion implantation [11]. A promising approach towards integration of the III–V or II–VI semiconductors with silicon technology is the direct growth of such QDs in silica or crystalline silicon. Depending on matrix and QDs types such systems can be used as LEDs, photodetectors or lasers operating in the large spectrum range starting from ultraviolet up to infrared. Tagliente et al. [12] successfully synthesized ZnO nanoparticles in SiO_2 film by ion implantation and annealing in oxidizing atmosphere for a tunable UV light emitter. The optical and microstructural properties of different QDs formed by sequential ion implantation into SiO_2 and AlO_2 matrices were investigated by Meldrum et al. [11]. The main problem that has to be solved in order to produce uniformly distributed nanoparticles with a small size deviation is the diffusion of implanted elements. Recently, Komarov et al. [13] synthesized InAs nanocrystals in Si by a high-temperature sequential ion implantation and long term fur-

S. Prucnal (✉) · M. Turek · A. Drozdziel · K. Pyszniak · J. Zuk
Maria Curie-Sklodowska University, Pl. M. Curie-Sklodowskiej 1, 20-035 Lublin, Poland
e-mail: s.prucnal@fzd.de

S. Prucnal · S.Q. Zhou · A. Kanjilal · W. Skorupa
Institute of Ion Beam Physics and Materials Research, Forschungszentrum Dresden-Rossendorf, P.O. Box 510119, 01314 Dresden, Germany

nace annealing. Such QDs preparation procedure involves a significant loss of implanted species and large variation of the QDs size.

In order to create the III–V semiconductor QDs homogeneously distributed in hosts and with small size deviation, diffusion coefficients of both elements has to be taken into account. One should be aware of the fact that the coefficient depends on the annealing time and temperature. In this work the optical properties of the InAs QDs formed in silicon by sequential ion implantation and flash lamp annealing (FLA) in the ms range are presented. The FLA has a big advantage on other annealing techniques due to the fact that during milliseconds annealing a silicon matrix is recrystallized, impurities are activated and out-diffusion of doped elements is suppressed [14, 15]. The PL spectrum shows intense luminescence, compared to that obtained from the one grown by the MBE technique [16], peaking at ∼1.3 μm and related to the InAs QDs with an average diameter of ∼7.5 nm.

2 Experimental details

Single-crystalline n-type (100) silicon wafers covered by 100 nm of a dry-grown thermal oxide layer were sequentially implanted with As and In ions using an ion source described in [17]. Initially the 170 keV As^+ ions were implanted with a fluence of 3.2×10^{16} ion/cm^2 and the implantation was performed at 500°C in order to initiate the clustering process of arsenic during ion implantation. Subsequently the samples were implanted by 240 keV In^+ ions with a fluence of 3×10^{16} cm^{-2} at room temperature. The expected impurity concentration is in the range of 5×10^{21} cm^{-3} at a depth of approximately 120 nm. The distribution of the implanted ions was first calculated by the SRIM-2007 code and confirmed by Rutherford Backscattering Spectrometry (RBS) investigation. The RBS spectra were collected with a collimated 1.7 MeV He^+ beam at a backscattering angle of 170°. After the implantation samples were annealed at different temperature and time in order to estimate the most suitable annealing conditions for InAs QDs formation. Three different annealing techniques were employed: furnace annealing at a temperature ranging from 700 up to 900°C for 30 min, rapid thermal annealing (RTA) at the same temperature range, but with 30 s and 1 min annealing times, and flash lamp annealing (FLA) with 600°C preheating and annealing temperature during FLA ranging from 700 up to 1200°C for 20 ms. In all cases samples were annealed in argon ambient. Cross-sectional transmission electron microscopy images were taken by means of an FEI Titan 80-300 scanning transmission electron microscope operating at 300 keV. The optical properties were investigated by μ-Raman Spectroscopy and low temperature photoluminescence (PL). The μ-Raman spectra were recorded at room temperature in the backscattering geometry in the range from 150 to 600 cm^{-1} using a 532 nm YAG laser. The PL spectra were recorded at the temperature range from 15 up to 300 K using a Jobin Yvon Triax 550 monochromator and a cooled InGaAs detector. For the sample excitation during the PL measurements a 405 nm laser beam of 20 mW power was applied.

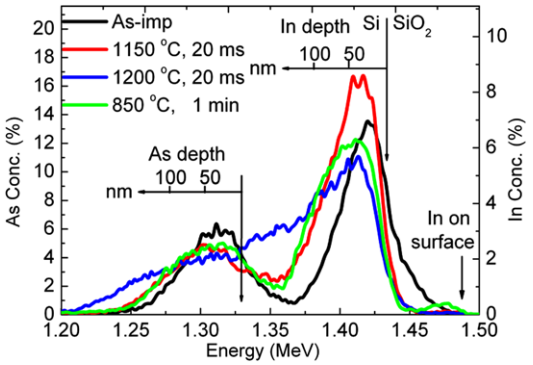

Fig. 1 RBS spectra of the As and In implanted and annealed samples

3 Results and discussion

Figure 1 shows As and In bands in the RBS spectra of the as-implanted and annealed samples at 1150 and 1200°C for 20 ms with 600°C preheating for 1 min (FLA) and annealed at 850°C for 1 min (RTA). The RBS measurements performed on the FLA samples annealed at temperatures up to 1100°C did not show diffusion of the implanted elements or the amount of the impurities which diffuse during the annealing is below the RBS sensitivity. The broadening of the As and In bands (which correspond to respective As and In depth profiles) is observed in case of the sample annealed at 1150°C for 20 ms or higher temperature. An increase of the annealing temperature up to 1200°C leads to relatively strong diffusion of both In and As into depth of silicon. It should be noticed that the depth profile of arsenic is much broader (even in the as-implanted sample) than that predicted from the SRIM code calculation due to the diffusion of arsenic during hot implantation process. The hot implantation of arsenic was chosen to initiate the clustering process of As already during ion implantation. The sample annealed at 850°C for 1 min exhibits not only diffusion of both elements into silicon but also strong out-diffusion of In atoms and its accumulation on the sample surface. In the case of 800°C for 30 min furnace-annealed sample (not shown here) less than 20% of In remains in the sample and indium precipitations are visible on the surface by a naked eye. A similar effect was observed by other researchers [13, 18].

Komarov et al. [13] have observed a strong reduction of the total amount of In and As in the sample annealed at

900°C for 45 min. The size of InAs nanoparticles, as obtained by TEM, was ranging from 2 up to 50 nm [13]. In our case the out-diffusion of In and As during furnace annealing can be additionally enhanced by oxygen. The diffusion of In and As in silica is much stronger than in silicon [19]. The results obtained by other researchers and our experimental data lead to the conclusion that the high-temperature long term processing by furnace annealing is not suitable for QD formation. Therefore, we have decided to introduce the FLA technique for QD processing in silicon. Nowadays the flash lamp annealing is successfully used for ultra-shallow junction [20] and silicon nanocrystal formation [21] or recrystallization of the amorphous silicon (a-Si) [15]. FLA is essentially a one-flash-one-wafer technique whose main attributes are the ease and control of processing over large wafer batches. The thermal budget introduced to the sample during FLA at 1100°C for 20 ms is sufficient to create InAs QDs, and to recrystallize amorphized silicon by annealing defects in the layer destroyed during ion implantation. On the other hand, the annealing time is too short to activate the diffusion of the implanted elements. Suzuki et al. [22] have investigated the diffusivity of arsenic in silicon during a solid-phase epitaxial (SPE) regrowth. They found that the regrowth speed of the amorphous layer during SPE is usually higher than impurity diffusion and increases with temperature much faster than diffusivity. Hence, the impurities are expected to be immobile during SPE and As is moving only together with amorphous/crystalline interface to the surface. The assumption of SPE as the recrystallization process in our case explains the absence of In and As diffusion in the sample during short time annealing.

Formation of the InAs QDs was confirmed by the μ-Raman spectroscopy. In as-implanted samples we have observed two broad bands at 150 and 460 cm^{-1}. These bands are associated with defects in the SiO_2 layer, mainly broken bonds between oxygen atoms (–Si–O··O–Si–, dots mean the broken bond) or highly elongated bonds which are created in silica during ion implantation [23, 24]. Moreover, the broad Raman band at 460 cm^{-1} is present in amorphous Si [25]. In the as-implanted sample, the peak at 520 cm^{-1} which is a fingerprint of crystalline silicon [26] vanishes completely. This observation indicates that during ion implantation a fully amorphized silicon layer was created. The broad band at 150 cm^{-1} still exists in the Raman spectra obtained from samples annealed at 700°C for 20 ms. At higher annealing temperature this band disappears from Raman spectra due to the annealed defects in silica. Simultaneously, the peak at 520 cm^{-1} emerges at the 700°C annealing which means that even in the case of such short annealing time and at a relatively low temperature, the process of silicon recrystallization starts. In case of the sample annealed at 850°C for 1 min, beside the 520 cm^{-1} Raman line two new peaks at about 215 and 235 cm^{-1} are visible. These new lines

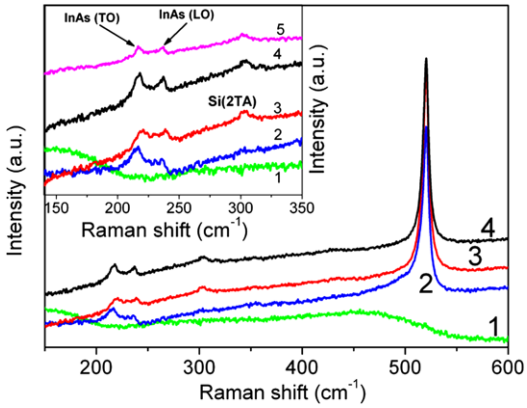

Fig. 2 μ-Raman spectra of In and As implanted samples annealed at 850°C for 1 min (2) and annealed for 20 ms at 1000°C (3), 1150°C (4), 1200°C (5). The spectrum of as-implanted sample (1) is shown as well. The *inset* shows a magnification of the 150–350 cm^{-1} spectral range

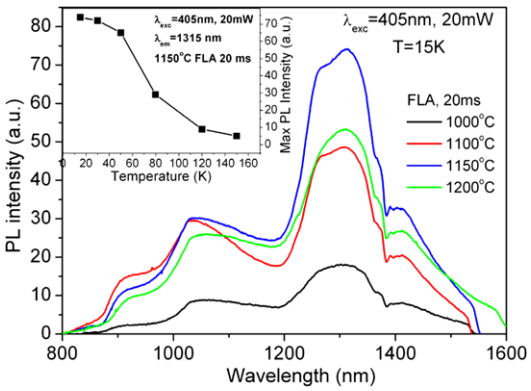

Fig. 3 15K PL spectra of the In and As implanted samples annealed at temperatures ranging from 1000°C up to 1200°C for 20 ms. The *inset* shows the intensity change of the 1315 nm peak corresponding to InAs QDs

are due to transverse optical (TO) and longitudinal optical (LO) phonons in InAs [27]. Their table values are: 217.3 and 238.6 cm^{-1}, respectively [26]. The lines are also observed in the case of samples annealed for 20 ms at a temperature above 1000°C, which directly proves the formation of the InAs QDs in silicon by flash lamp annealing. An additional peak at 300 cm^{-1} was observed for the samples annealed at a temperature higher than 1000°C, and originates from the second-order two transverse acoustic phonon (2TA) scattering from crystalline Si substrates.

Figure 3 shows the PL spectra taken from samples implanted with In and As and subsequently annealed at different temperatures ranging from 1000°C up to 1200°C for 20 ms with tree main bands at about 910, 1035 and 1300 nm. The PL bands with maxima at 910 and 1035 nm are due to radiative recombination of photo-excited carriers in the amorphous phase of the microcrystalline silicon (μc-Si) [28]. The PL intensity drop around 1390 nm is due to water vapor absorption [29]. The detailed study of the PL

and Raman spectra shows that the high-temperature flash lamp annealing of the amorphized silicon during ion implantation leads to μc-Si formation. The main infrared PL band at around 1300 nm is obtained from the InAs nanodots. In the light of the Raman spectroscopy results, the absence of this band in the unimplanted samples and annealed at the same conditions, as well as in the samples annealed at temperatures below 900°C for 20 ms, it is assumed that this band corresponds to crystalline InAs QDs with the average diameter of about 7.5 ± 0.5 nm [30].

We have found that the minimum annealing temperature needed for the crystalline InAs QDs formation in Si matrix is around 1000°C for the FLA (annealing time 20 ms). The strongest PL signal from InAs QDs was obtained from the sample annealed at 1150°C for 20 ms. Annealing at higher temperature leads to a strong diffusion of the implanted elements and a decrease of the PL efficiency. Moreover, the sample annealed at 850°C for 1 min exhibits two peaks in the Raman spectrum corresponding to the InAs composition but did not show a clear PL signal at 1300 nm. This leads to the conclusion that after such a thermal treatment the InAs clusters are formed, but they are either amorphous or contain many defects which introduce nonradiative de-excitation channels to the quantum dots. Also the samples annealed at temperatures below 1000°C for 20 ms did not show luminescence related to the InAs QDs. The inset in Fig. 3 shows the change of the maximum PL intensity monitored at 1315 nm with the measurement temperature. The PL signal from the InAs QDs was visible for the temperature up to 150 K and the maximum peak position shows red shift of about 10 nm with the increasing temperature from 15 to 150 K. For higher sample temperatures only the luminescence originating from μc-Si was detected.

In addition the HRTEM investigation of the As and In implanted and annealed samples were performed. The sample annealed at 850°C for 1 min shows formation of the InAs quantum dots in silicon with average diameter of 10 nm. The QDs are crystalline but strongly strained and contains many defects what explains absence of luminescence. Moreover, small pyramidal shaped and crystalline indium nanodots on the SiO_2 surface were found (see inset Fig. 4a). In the case of flash lamp annealed samples good quality InAs nanocrystals start to grow at temperature higher then 900°C and they are located on both sides of the SiO_2/Si interface with average size of 7.5 nm. The lattice constant of the InAs nanocrystals increases from 6.048 to 6.055 Å with increasing the annealing temperature from 1000 to 1200°C due to the network relaxation and they are oriented with their (001) planes parallel to the Si (001) planes. After annealing at 1150°C for 20 ms the InAs nanoparticles are crystalline, no matter where they are formed in silicon or in silica (see Fig. 4b). Interesting is that the annealing at 1200°C for the same duration time leads to formation mainly amorphous InAs QDs in silica and crystalline one in silicon (not shown here) what explains the decrease of the PL intensity with increasing the annealing temperature above 1150°C.

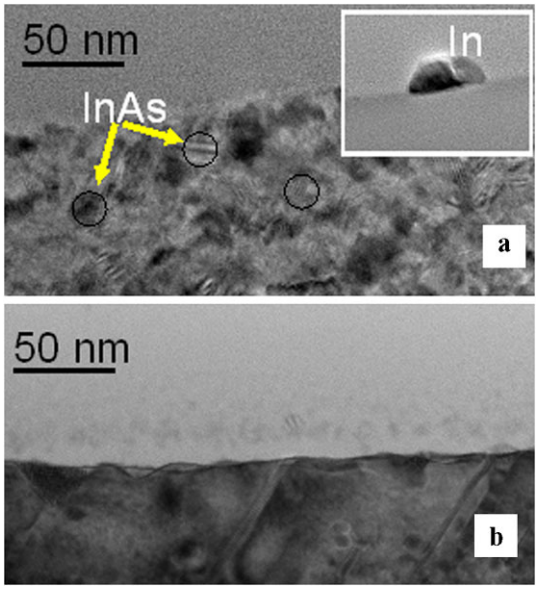

Fig. 4 HRTEM image of the sample annealed at 850°C for 1 min (**a**) and 1150°C for 20 ms (**b**). The *inset* shows the pyramidal shape of crystalline indium island formed on the SiO_2 surface

4 Conclusions

We have successfully synthesized InAs QDs by sequential ion implantation and flash lamp annealing. The PL and μ-Raman measurements prove the formation of the InAs QDs in the silicon matrix with an average size of 7.5 ± 0.5 nm. After FLA the silicon layer amorphized during the ion implantation is recrystallized and μc-Si is formed. Moreover, millisecond range thermal processing suppresses the diffusion of the implanted elements what makes the InAs QD formation more effective. According to our results Si with direct band gap InAs QDs is a potential candidate for efficient Si-based LEDs.

Acknowledgement This work was financially supported by the Polish Ministry of Science and Higher Education, Grant No. 2466/B/T02/2009/37.

References

1. L.E. Brus, J. Chem. Phys. **80**, 4403 (1984)
2. T. Canham, Appl. Phys. Lett. **57**, 1046 (1990)
3. S. Sapra, D.D. Sarma, Phys. Rev. B **69**, 125304 (2004)
4. J. Valenta, N. Lalic, J. Linnros, Appl. Phys. Lett. **84**, 1459 (2004)
5. J.H. Chen, T.F. Lei, D. Landheer, X. Wu, M.W. Ma, W.C. Wu, T.Y. Yang, T.S. Chao, Jpn. J. Appl. Phys. **46**, 6586 (2007)
6. X.J. Hao, E.-C. Cho, C. Flynn, Y.S. Shen, S.C. Park, G. Conibeer, M.A. Green, Sol. Energy Mater. Sol. Cells **93**, 273 (2009)

7. M.D. Dvorak, B.L. Justus, D.K. Daskill, D.G. Hendershot, Appl. Phys. Lett. **66**, 804 (1995)
8. T. Shmizu-Iwayama, K. Fujita, S. Nakao, K. Saitoh, T. Fujita, N. Itoh, J. Appl. Phys. **75**, 7779 (1994)
9. R. Ding, H. Wang, H. Yang, W. She, Z. Qiu, L. Luo, W.F. Lau, W.Y. Cheung, S.P. Wong, Mater. Chem. Phys. **76**, 262 (2002)
10. R.L. Wells, S.R. Aubuchon, S.S. Kher, M.S. Lube, Chem. Mater. **7**, 793 (1995)
11. A. Meldrum, L.A. Boatner, C.W. White, Nucl. Instrum. Methods Phys. Res. B **178**, 7 (2001)
12. M.A. Tagliente, M. Massaro, G. Mattei, P. Mazzoldi, V. Bello, G. Pellegrini, J. Appl. Phys. **104**, 093505 (2008)
13. F. Komarov, L. Vlasukova, W. Wesch, A. Kamarou, O. Milchanin, S. Grachnyi, A. Mudryi, A. Ivaniukovich, Nucl. Instrum. Methods Phys. Res. B **266**, 3557 (2008)
14. F. Lanzerath, D. Buca, H. Trinkaus, M. Goryll, S. Mantl, J. Knoch, U. Breuer, W. Skorupa, B. Ghyselen, J. Appl. Phys. **104**, 044908 (2008)
15. B. Pétz, L. Dobos, D. Panknin, W. Skorupa, C. Lioutas, N. Vouroutzis, Appl. Surf. Sci. **242**, 185 (2005)
16. G.E. Cirlin, V.G. Dubrovskii, V.N. Petrov, N.K. Polyakov, N.P. Korneeva, V.N. Demidov, A.O. Golubok, S.A. Masalov, D.V. Kurochkin, O.M. Gorbenko, N.I. Komyak, V.M. Ustinov, A.Yu. Egorov, A.R. Kovsh, M.V. Maximov, A.F. Tsatsul'nikov, B.V. Volovik, A.E. Zhukov, P.S. Kop'ev, Zh.I. Alferov, N.N. Ledentsov, M. Grundmann, D. Bimberg, Semicond. Sci. Technol. **13**, 1262 (1998)
17. M. Turek, S. Prucnal, A. Drozdziel, K. Pyszniak, Rev. Sci. Instrum. **80**, 043304 (2009)
18. A.L. Tchebotareva, J.L. Brebner, S. Roorda, C.W. White, Nucl. Instrum. Methods Phys. Res. B **175–177**, 187 (2001)
19. D.A. Antoniadis, I. Moskowitz, J. Appl. Phys. **53**, 9214 (1982)
20. W. Skorupa, T. Gebel, R.A. Yankov, S. Paul, W. Lerch, D.F. Downey, E.A. Arevalo, J. Electrochem. Soc. **152**, G436 (2005)
21. G.A. Kachurin, I.E. Tyschenko, K.S. Zhuravlev, N.A. Pazdnikov, V.A. Volodin, A.K. Gutakovsky, A.F. Leier, W. Skorupa, R.A. Yankov, Nucl. Instrum. Methods Phys. Res. B **122**, 571 (1997)
22. K. Suzuki, Y. Kataoka, S. Nagayama, Ch.W. Magee, T.H. Büyüklimanli, T. Nagayama, IEEE Trans. Electron. Devices **54**, 262 (2007)
23. G.E. Walter, P.N. Krishnan, S.W. Freiman, J. Appl. Phys. **52**, 2832 (1981)
24. Y. Hibino, H. Hanafusa, K. Ema, S. Hyodo, Appl. Phys. Lett. **47**, 812 (1985)
25. J.E. Smith Jr., M.H. Brodsky, B.L. Crowder, M.I. Nathan, A. Pinchuk, Phys. Rev. Lett. **26**, 642 (1971)
26. W. Martienssen, H. Warlimont (eds.), *Springer Handbook of Condensed Matter and Materials Data* (Springer, Berlin, 2005)
27. M.Yu. Ladanov, A.G. Milekhin, A.I. Toropov, A.K. Bakarov, A.K. Gutakovskii, D.A. Tenne, S. Schulze, D.R.T. Zahn, J. Exp. Theor. Phys. **101**, 554 (2005)
28. M. Yamaguchi, K. Morigaki, J. Phys. Soc. Jpn. **62**, 2915 (1993)
29. C.J. Patel, Q.X. Zhao, O. Nur, M. Willander, Appl. Phys. Lett. **72**, 3047 (1998)
30. J.-W. Luo, A. Franceschetti, A. Zunger, Nano Lett. **8**, 3174 (2008)